Augmenting Radar Doppler Resolution with Neural Networks

Jabran Akhtar
Norwegian Defence Research Establishment (FFI), Kjeller, Norway
Email: jabran.akhtar@ffi.no

***Abstract*—In order to generate high-resolution Doppler profiles a radar needs to emit a large number of pulses within a coherent processing interval (CPI). For a radar operating in demanding scenarios it can be difficult to sustain a long CPI across search directions. In this work, an application of small neural networks is proposed to augment the Doppler resolution beyond the one detailed by basic radar parameters. A specific neural network structure is proposed which can be trained to operate on complex valued time-domain data and yield a frequency transformed output with an increased Doppler bin resolution. It is shown that by making use of these techniques a radar can improve its ability to detect targets and to distinguish closely spaced targets. A limited increase in the Doppler bin resolution can be sustained with little to no negative impact on the false alarm rate.**

***Keywords*—Radar, range-Doppler, constant false alarm rate (CFAR), discrete Fourier transform, neural networks**

I. Introduction

The construction of range-Doppler maps constitutes a basic but an important middle step in radar signal processing. Transforming slow-time radar data into Doppler domain offers integration gain and, simultaneously, targets with distinct velocities can be differentiated from each others. Nevertheless, in order to construct high-resolution range-Doppler maps the radar needs to transmit a large number of pulses within a coherent processing interval (CPI) as the number of bins representing the Doppler domain complements the number of emit pulses [1], [2].

In order to improve upon the resolution of range-Doppler maps a variety of methods have been proposed in the literature. Many of the techniques look at bandwidth extrapolation of emit pulses while other aim for more versatile form of filtering [3], [4], [5]. In other contexts, several deep learning methods have been developed for super-resolution image reconstruction [6], [7]. Super-resolution being defined as a resolution beyond the original capability of the sensors hardware. The application of these methods in radars have though been very limited which can be attributed to the specific properties of radar data and the required characteristics of range-Doppler maps. A high-resolution map is simply not very practical if it also results in an enlarged false alarm rate though these aspects have not been addressed in details by current research. In [8], a neural network based technique was proposed to generate range-Doppler maps following the framework of a compressed sensing radar (CS) and sparse reconstruction (SR). The radar was assumed to collect data in a non-coherent CS mode with inherent gaps and the neural networks were trained to generate range-Doppler images, range bin by range bin, as under SR [9], [10]. This was shown to work well although the reconstructed range-Doppler maps were not fully sparse but contained low-level noise. The other main disadvantage with this approach is that the collected data would need to have gaps within it and SR can be seen as a detection process in itself which is not always desirable. More importantly, although the notion of a CS radar is attractive and provides theoretical guarantees for when the reconstruction process will converge, many radar systems may not operate in such a mode which necessitates the development of alternative methods for Doppler bin resolution enhancement.

This work can be seen as complementing [8] and exploring the other point of view where the new objective is to feed a coherent set of limited slow-time data into small neural networks in an attempt to obtain high-resolution Doppler profiles for each range bin. The network must thus learn to extrapolate time-domain data with respect to targets and inherently perform a tapered Fourier transform in the same process. High-resolution range-Doppler maps would in principle allow for supplementary integration gain and can therefore be beneficial for detection of weak targets as long as a low false alarm rate can be maintained. Further on, a more accurate target placement with regard to Doppler bins allows constant false alarm rate (CFAR) detectors to discriminate between targets who may otherwise mask each other out.

Although machine learning has been in much focus over the last years, *training* an artificial fully-connected neural network to yield a complete discrete Fourier transform has been seen as an intricate task and no clear learning strategy has been proposed in the literature. It turns out that in order to design neural networks to accomplish the aforementioned process, the neural networks must be tailored to take account of the large variation in the dynamic levels of slow-time data and such a design is presented in this paper. To evaluate the outcomes, the detectional capabilities of the generated range-Doppler maps are thoroughly investigated in simulated scenarios with single and multiple targets under standard CFAR detection schemes.

II. System model

In this text we assume a classical radar operating mode where M pulses are emit towards a set direction in a CPI. The targets are modeled as slowly fluctuating with Swerling 1 distribution where the values vary randomly between dwells but with a given mean signal-to-noise ratio (SNR) per pulse. The collected slow-time data is presumed to be represented by a complex matrix $\mathbf{S} \in \mathbb{C}^{M \times R}$ where the columns indicate slow-time pulses while the rows the R range bins (fast-time). For each CPI, the processing unit performs an independent tapered Fourier transform over each range bin to construct a range-Doppler map $\mathbf{D} \in \mathbb{C}^{M \times R}$. Targets exhibiting a constant radial velocity thus emerge concentrated in a range-Doppler map.

To search for targets, each individual cell of the range-Doppler map is assumed evaluated one by one through the cell averaging (CA)-CFAR detector. The detector takes the point-wise square law samples of the image $\hat{\mathbf{D}}$, $\hat{\mathbf{D}} = |\mathbf{D}|.^2$, and a sliding window of size $2N+2G+1$ is moved across excluding the edges. The $2N+2G+1$ samples in range specified by the window are extracted in $x(u) = \hat{\mathbf{D}}(t-N-G : t+N+G, \omega)$, for a given $1+N+G \leq t \leq R-N-G$, $1 \leq \omega \leq M$ and $u = 1, 2, ..., 2N+2G+1$. The cell in the middle of the window, $x(N+G+1)$, cell under test (CUT), is compared against a scaled average, γ. G gap cells immediately to the right and left of CUT are discarded and a detection is declared if

$$x(u)_{|u=CUT} > \gamma\, K, \tag{1}$$

where K is a set threshold. The background average, γ, in CA-CFAR is computed by making use of all $2N$ reference cells across the range dimension, $\gamma = \frac{1}{2N}(\sum_{k=1}^{N} x(k) + \sum_{k=N+2G+2}^{2N+2G+1} x(k))$. The underlying issue with many CFAR techniques, including CA-CFAR, is the inability to retain a satisfactory performance in the presence of other targets in the reference cells. This is particularly a problem if the number of Doppler bins, M, is small as auxiliary targets will often end up in identical bins due to poor resolution.

A. Neural network training and processing

In order to increase the Doppler resolution beyond the basic M bins a machine learning approach based on neural networks can be put forward assuming that the maximum number of targets at a range bin is limited under an established noise floor. The networks will be trained to take M slow-time samples for a given range bin and output $M+L$ samples in frequency domain, $L \geq 2$ being an even number. By performing this operation across all range bins a high-resolution range-Doppler map $\hat{\mathbf{D}} \in \mathbb{C}^{M+L\times R}$ can in principle be constructed. An optional tapering function is also presumed incorporated in the neural network training and the slow-time data fed into the network is from the middle of the set; with the equivalent slow-time extrapolation of $L/2$ samples occurring at both edges. Tapering functions are useful in reducing sidelobe leakages but the downweighting of data at both ends also reduces the amount of effective information which is extracted by the Fourier transform. In this regard, even a somewhat inaccurate extrapolation process can still be useful in a radar detectional system as long as the detection rate improves without a false alarm rate degradation.

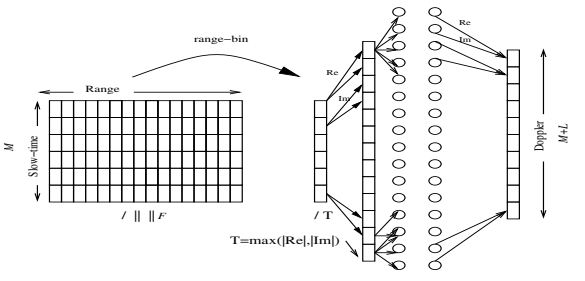

Fig. 1: Illustration of the data and network structure

To train a neural network for the designated task, we assume that a set of P slow-time data matrices corresponding to different CPIs with $M+L$ pulses have been collected, $\mathbf{S}_1$, ..., $\mathbf{S}_P \in \mathbb{C}^{M+L\times R}$. The main parameters such as the tapering function, M and L are expected to be known and fixed for a given network. To accurately train the network, the range bin data which is the input to the neural network and the Doppler output profile should contain various type of signals. We categorize the two main classes as

- range bin containing targets
- range bin containing only noise.

Noise-only bins constitute learning with respect to the noise floor. In addition to that, range bins with targets should contain multiple targets at different randomly selected velocities; training on up to two targets normally leads to satisfactory outcomes with well-generalized networks as will be shown later and was demonstrated in [8].

To construct the database for network training we first curtail the slow-time matrices from $M+L$ pulses to M pulses by only retaining the M middle values, $\mathbf{S}_l^* = \mathbf{S}_l(:,\ L/2 : M+L/2) \in \mathbb{C}^{M\times R}$, $l = 1, ..., P$. Both the full $\mathbf{S}_l$ and the downsized $\mathbf{S}_l^*$ slow-time matrices are normalized by the Frobenius norm of the reduced matrix, $\bar{\mathbf{S}}_l^* = \mathbf{S}_l^*/||\mathbf{S}_l^*||_F$ and $\bar{\mathbf{S}}_l = \mathbf{S}_l/||\mathbf{S}_l^*||_F$. The objective is to reduce the upper dynamic range and the corresponding range-Doppler map generated from $\bar{\mathbf{S}}_l$, incorporating any tapering, is denoted by $\bar{\mathbf{R}}_l \in \mathbb{C}^{M+L\times R}$. In the next step, a random range bin r is selected and M complex-valued samples are extracted $\mathbf{s} = \bar{\mathbf{S}}_l^*(:, r)$ alongside the reciprocal $M+L$ complex Doppler profile samples from $\mathbf{r} = \bar{\mathbf{R}}_l(:, r)$. The input $\mathbf{s}$ and output $\mathbf{r}$ for a given range bin is complex valued and to utilize real valued neural networks the data is split in two, a real and an imaginary part, $\tilde{\mathbf{s}} = [\Re(\mathbf{s}),\ |\Im(\mathbf{s})]$ and $\tilde{\mathbf{r}} = [\Re(\mathbf{r}),\ |\Im(\mathbf{r})]$. As it will be shown, this can serve quite well and does not necessitate the use of complex valued networks [11]. Before passing on to the neural network, the input data for each range bin must further be normalized and for this we utilize maximum absolute normalization. The $2M$ samples are normalized by the largest absolute value among them,

$$T = \max\left(|\tilde{\mathbf{s}}|\right). \tag{2}$$

The input $\mathbf{x}$ to the neural network is thus defined as $\mathbf{x} = [\frac{1}{T}\tilde{\mathbf{s}}\ \ T]$. The largest absolute input value to the network (excluding T) will thus always equal one while the lowest figure remains undefined. The normalization factor T is also fed into the neural network to incorporate rescaling in the same learning procedure. Notice that the overall structure therefore becomes quite different from the one of [8] as the network is now given the additional responsibility to output the Doppler profile with correct calibration. The overall process can be described through $\tilde{\mathbf{r}} = f(\mathbf{x})$ where $f()$ corresponds to the fully-connected feedforwarding network neural network as a function with $f:\ 2M+1 \rightarrow 2(M+L)$. The process is depicted in figure 1 and each node is assumed to utilize the $tanh$ activation function. For the training process, multiple samples from arbitrary range bins should be taken, however, an important objective must be to preserve the false alarm level in the process. It is therefore important that the network learns to recognize instances of noise and thereupon only outputs transformed variants of noise. Weighting can be utilized to accomplish this, where the training database encloses a greater occurrences of range bins only consisting of noise.

Normalization of slow-time data, first collectively across the matrix, and then per range bin plays a key role for successful training of the network and the ability to transform slow-time data into frequency domain. The performance of the trained networks will nevertheless depend on several factors such as the size of the database, the depth and width of the neural network and not least the choice of L. Training on a neural network with the size of at least two hidden $tanh$ layers, one linear output layer and three to five times the nodes in each layer as the number of output entries generally results in satisfactory convergence and applicable performance. As L is increased, the convergence will eventually start to degrade as the network may start to generate an inflated noise floor level and extrapolate at incorrect frequency bins mistaking noise for potential targets. Detailed examples of these aspects are provided next.

III. Simulation examples

In this section we present a number of examples and simulation results to concertize how the presented concept can be put to use and what type of detectional advantages can be expected. For the simulated training example we assume a radar setup with 1000 simulated range bin. 30 targets are randomly situated within this region while another 20 targets are placed in the same range bins as already occupied by others (i.e. up to two targets per range bin). The target velocity is in all cases randomly determined between -75m/s and 75m/s. The targets fluctuate randomly from dwell to dwell but otherwise retain the power level with the single pulse SNR varying between -25dB to 30dB. The targets are also assumed to spread across both neighboring range bins with sidelobes of -20dB. With a probability of 0.5, a target spread is modeled where an adjacent range cell is instead modeled as an independent target. The Chebyshev window with 100 dB of sidelobe attenuation is applied in all instances before the Fourier transform. Figure 2 illustrates such a simulated range-Doppler map with the CPI interval of $M = 6$. This exact example was not used for training but represents a typical range-Doppler map and the corresponding slow-time data from random range bins would constitute parts of the input for the training database. In this regard, figure 3 shows the range-Doppler map for the same set but assuming $M = 10$ which would designate the output. By comparing these two figures it is apparent that even with two additional data samples the Doppler spread is narrower permitting a more accurate Doppler placement.

Several neural networks were trained assuming $M = 6$ or $M = 12$ and varying L from 2 to 6 (8 for $M = 12$) with training over 500000 epochs using the scale conjugate gradient algorithm. For each training session, 50000 arbitrary profiles were collected only containing white Gaussian noise from randomly generated 504 range-Doppler maps while another 10000 profiles contained noise and targets with varying SNR. A larger ratio, such as 5:1 between the categories, turns out to be an important factor for proper handling of noise-only range bins. The data was put to use for training as a single batch. The fully-connected feedforwarding network contained two hidden layers with $5 \times 2 \times (M + L)$ nodes in each layer corresponding to five times the nodes as the number of inputs and the two times factor accounting for the real and imaginary parts. The maximum value of T achieved during he training process was determined to be 0.22.

A. M=6

The error rates after training for $M = 6$ are given in table I[1]. Also provided on the right is the average relative error norm between 100 randomly range-Doppler images when the learned network was fed untrained simulated data and compared with images assuming full availability of $M + L$ pulses. From the table, it is evident that as L increases the approximation starts to degrade; this should be expected as the network may start to assume noise for targets while extracting weak targets based on very few pulses is otherwise a challenging task. Nevertheless, the approximation is reasonable for small values of L.

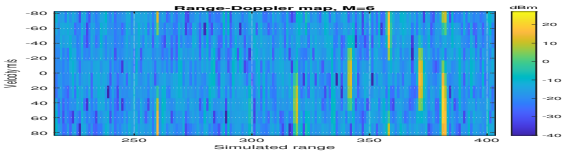

Fig. 2: R-D map for training and evaluation $M = 6$

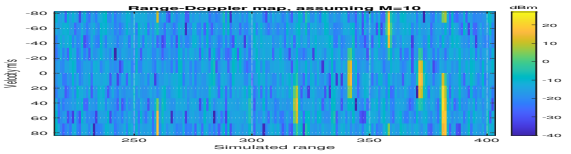

Fig. 3: R-D map for training and evaluation $M = 10$

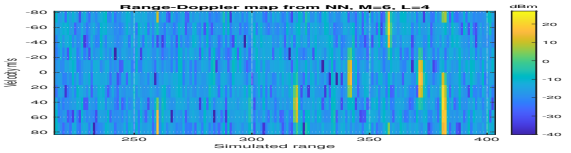

Fig. 4: R-D map from neural network, $M = 6, L = 4$

L	Training error	Relative error test images
2	$2.84 \cdot 10^{-8}$	0.010
4	$1.69 \cdot 10^{-7}$	0.032
6	$4.78 \cdot 10^{-7}$	0.071

TABLE I: Performance evaluation for $M = 6$

As an illustrative example, by taking the same $M = 6$ pulses employed for figure 2 and feeding them through the trained network for $M = 6$ and $L = 4$ returns the range-Doppler map shown in figure 4. Visually, the result is very similar to figure 3 generated from a full set of 10 pulses and all the targets exhibit a comparable restricted Doppler spread. The relative error norm between the two images $||R_F - R_{NN}||_F / ||R_F||_F$ comes to 0.0037 where R_F corresponds to the image generated from complete set of 10 pulses where R_{NN} reflects the image generated from trained neural network. The small error norm and the visual similarity demonstrating clear benefits for confined Doppler resolution enhancement. Nevertheless, to fully characterize the performance from neural networks detail simulations need to be carried out with respect to probability of detection (P_D) and false alarm rate (P_{FA}).

In a radar detectional context, the most important properties of range-Doppler maps are linked with the ability to detect tar-

[1]The trained neural networks are available for download from: https://doi.org/10.6084/m9.figshare.14540232

gets. To investigate the performance of trained neural networks we consider two different scenarios. For the first scenario, only a single target is simulated in the full range-Doppler map, permitting a careful characterization of individual target detection and false alarm rate in white noise at different SNRs. CA-CFAR is employed for detection with $N = 3$ guard cells and $G = 8$ reference cells on both sides of the sliding window. The detection threshold is set at $K = 12$dB and a clustering of targets is performed if positive detection occurs due to target spread in either Doppler or range. Targets are only grouped together if there is a consecutive set of detections without any gaps. Probability of detection is defined as the number of correctly detected targets relative to the total number of simulated targets after grouping while false alarm rate as the number of incorrectly detected targets in relation to total number of tests. The evaluation was carried over 450 new range-Doppler maps representing about 4.4 millions CFAR tests.

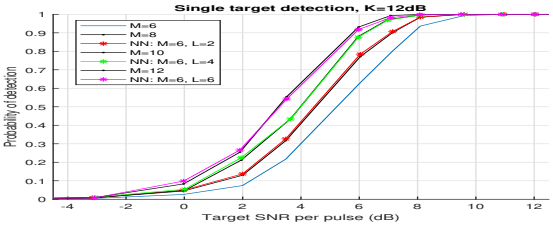

Fig. 5: Probability of detection, single target, $M = 6$

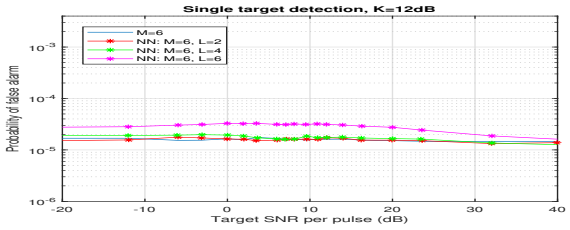

Fig. 6: False alarm rate, single target, $M = 6$

The P_D curves are depicted in figure 5 and it is evident that the application of trained neural networks improves the system's capacity to detect targets. Starting from $M = 6$, the neural network for $M = 6, L = 2$ (red curve) manages to approximate the same performance as if the radar had utilized 8 full pulses (black dotted). These two curves overlap perfectly and the improvement is consistent throughout the SNR range. The identical situation can be observed for the cases of $M = 6, L = 4$ (green curve) and $M = 6, L = 6$ (magenta curve). Although the P_D performance is very good, an enlarged L does come at the expense of a higher false alarm rate as can be observed in figure 6. The false alarm rate is comparable to the standard case of $M = 6$ for $M = 6, L = 2$ but is marginally increased for $L = 4$. With $L = 6$, the increase in the false alarm is more noticeable and one would need to weight the trade-off between the ability to detect more targets at the expense of a higher false alarm rate.

The curves in figure 5 provide the detectional capability if the range-Doppler map only contains a single target. In the second simulation scenario, 50 targets were randomly placed in the range-Doppler map, as described for the training process, to investigate the impact of closely spaced targets. For the evaluation, all 50 targets had the same SNR. In this regard, figure 7 provides the CA-CFAR detection rates which evidently also improve with neural networks. Notice that the P_D never exactly reaches 1 as with random target placement there always will be targets close to each other in range and with a velocity resulting in identical Doppler bins. With better resolution in Doppler the probability of the targets ending up in the same velocity bin diminishes and this advantage remains effective even at high SNR values. Although the extrapolation of e.g. only two pulses may initially seem modest, the impact of this can still be compelling and corresponds to one third additional data which can be critical for radars operating with stringent timing and transmission constrains.

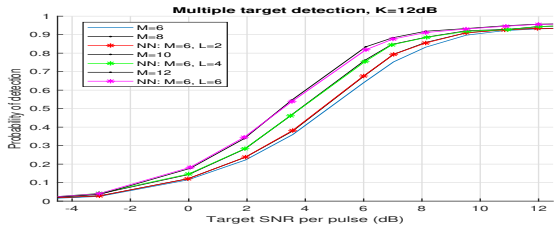

Fig. 7: Probability of detection, multiple targets, $M = 6$

B. M=12

The simulations from the above section were replicated for the case of $M = 12$ trained networks. The comparable error rates are given in table II and exhibit much better training efficiency as more data is initially available. The final P_D curves can be examined in figure 8 and the P_{FA} plot in figure 9 for a single target scenario. As with the previous case, the P_D improvement of the neural network with $M = 12$ and $L = 2$, $L = 4$, $L = 6$ or $L = 8$ is in line with if the radar had full access to, respectively, either $M = 14, 16, 18$ or 20 pulses. The networks thus exhibit good ability to extract weak targets. As a trade-off, the false alarm rate increases with greater values of L but two to four pulse extrapolation is a very viable option without any significant degradation of the system's P_{FA} level. In contrast to the earlier situation of $M = 6$ the increase in the false alarm now occurs at high SNR values and can mostly be attributed to the fact the Doppler target spread at large SNR breaks up and no longer results in consecutive CFAR detections, an example of this is provided in figure 10 where one can also notice the elevated noise floor. This detection issue can potentially be solved by more advanced clustering algorithms or by not applying the neural networks for range bins where targets already stand out with high SNR. These aspects are though not discussed further in this text.

L	Training error	Relative error test images
2	$1.22 \cdot 10^{-9}$	0.008
4	$4.87 \cdot 10^{-9}$	0.014
6	$2.09 \cdot 10^{-8}$	0.032
8	$6.50 \cdot 10^{-8}$	0.060

TABLE II: Performance evaluation for $M = 12$

Altogether, the result indicate the ability of appropriately designed and trained neural networks to extract information from available slow-time data. As an alternative interpretation, the proposed networks can be seen as a technique to mitigate the impact of tapering functions on the signal edges.

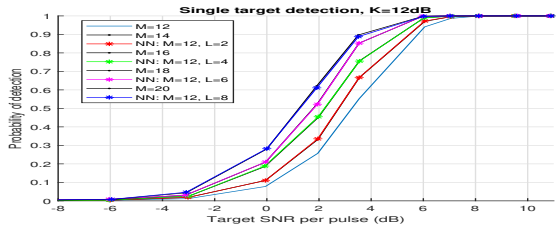

Fig. 8: Probability of detection, single target, $M = 12$

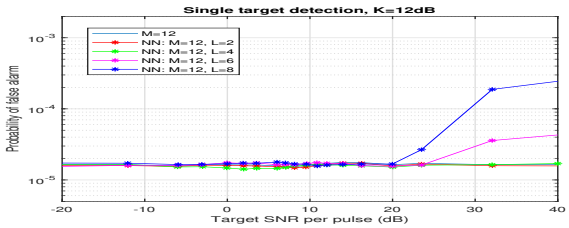

Fig. 9: False alarm rate, single target, $M = 12$

C. Visual exemplification

The above sections have emphasized the CA-CFAR detection capabilities of range-Doppler maps where the profiles are generated through trained neural networks. In other applications, such as micro-Doppler extraction, target imaging or recognition. detection in itself is not of primarily interest. The proposed networks have a potential usage in these circumstances as an alternative to the Fourier transform for generation of high-resolution images. To demonstrate this, a series of test signals were generated over 100 simulated range bins. On the left hand side, two targets were incorporated in each range bin, the first target with a sweeping velocity and decreasing power while the second target exhibits constant zero Doppler but increasingly energy level. In the second half of range bins, a third target was introduced (even though the network was not trained under more than two targets).

The left image in figure 11 depicts the standard range-Doppler image with $M = 12$ while the middle image assumes full availability of $M = 18$ pulses. The right side shows the result from the trained network for $M = 12, L = 6$. The targets are easily identifiable and highly concentrated in Doppler for all velocities and intensities compared to the original image with only $M = 12$ pulses. This example is provided for illustration purposes only but demonstrates

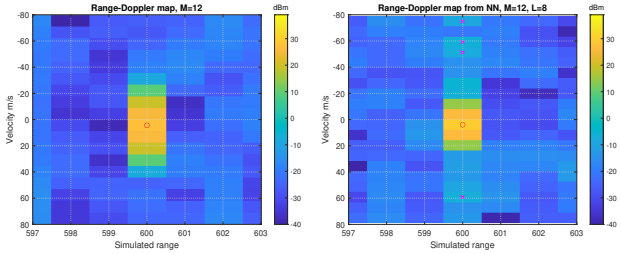

(a) $M = 12$ (b) $M = 12, L = 8$

Fig. 10: Excessive extrapolation example for a single target. On the right side the target Doppler spread results in unconnected CFAR detections (crossed).

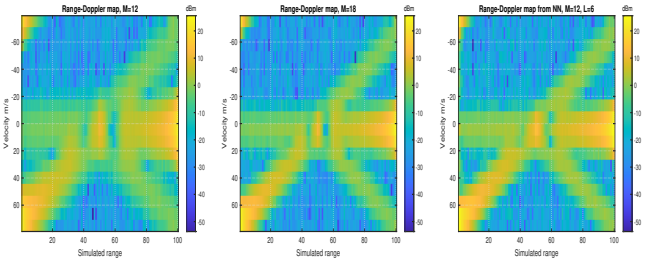

(a) $M = 12$ (b) $M = 18$ (c) $M = 12, L = 6$

Fig. 11: Illustration of image regeneration

how higher resolution range-Doppler images can easily be generated by taking advantage of small neural networks even though the CFAR process may yield suboptimal outcomes.

IV. Conclusion

This paper proposed the application of small neural networks to generate high-resolution Doppler profiles of radar signals. In a data starved environment, a radar may only be able to transmit a limited amount of pulses, resulting in a low Doppler resolution and restricted ability to distinguish between closely spaced targets. It was shown that fully-connected feedforwarding neural networks can successfully be trained to take slow-time time-domain data as an input and return high-resolution frequency profiles as output. The detectional performance was shown to be equivalent to the case of full data availability. As a trade-off, the process can potentially result in a higher false alarm rate, though for moderate Doppler bin resolution enhancement the original levels can be conserved.

References

[1] N. Levanon, *"Radar Principles"*. New York: Wiley, 1988.

[2] R. J. Sullivan, *"Microwave radar, imaging and advanced concepts"*. Artech House, 2000.

[3] L. Chen and J. Chen, "High resolution radar imaging using bandwidth extrapolation," in *International Congress on Image and Signal Processing*, 2010, pp. 3591–3595.

[4] A. Gupta, U. Madhow, and A. Arbabian, "Super-resolution in position and velocity estimation for short-range MM-wave radar," in *Proc. of Asilomar Conference on Signals, Systems and Computers*, 2016, pp. 1144–1148.

[5] K. Armanious, S. Abdulatif, F. Aziz, U. Schneider, and B. Yang, "An adversarial super-resolution remedy for radar design trade-offs," in *European Signal Processing Conference*, 2019.

[6] W. Yang, X. Zhang, Y. Tian, W. Wang, J.-H. Xue, and Q. Liao, "Deep learning for single image super-resolution: A brief review," *IEEE Transactions on Multimedia*, vol. 21, no. 12, Dec. 2019.

[7] J. Gao, B. Deng, Y. Qin, H. Wang, and X. Li, "Enhanced radar imaging using a complex-valued convolutional neural network," *IEEE Geoscience and Remote Sensing Letters*, vol. 16, no. 1, pp. 35–39, Jan. 2019.

[8] J. Akhtar, "Sparse range-Doppler image construction with neural networks," in *Proc. of IEEE Radar Conference*, 2020, pp. 291–296.

[9] D. Cohen and Y. C. Eldar, "Reduced time-on-target in pulse Doppler radar: Slow time domain compressed sensing," in *Proc. of IEEE Radar Conference*, 2016.

[10] J. Akhtar and K. E. Olsen, "Formation of range-Doppler maps based on sparse reconstruction," *IEEE Sensors Journal*, vol. 16, no. 15, pp. 5921–5926, Aug. 2016.

[11] O.-L. Ouabi, R. Pribic, and S. Olaru, "Stochastic complex-valued neural networks for radar," in *European Signal Processing Conference*, 2020, pp. 1442–1446.